International Journal of Electrical, Electronic and Communication Sciences
ISSN: 2517-9438
Vol:3, No:8, 2009

Effective Image and Video Error Concealment using RST-Invariant Partial Patch Matching Model and Exemplar-based Inpainting

Shiraz Ahmad and Zhe-Ming Lu, *Senior Member, IEEE*

Abstract—An effective visual error concealment method has been presented by employing a robust rotation, scale, and translation (RST) invariant partial patch matching model (RSTI-PPMM) and exemplar-based inpainting. While the proposed robust and inherently feature-enhanced texture synthesis approach ensures the generation of excellent and perceptually plausible visual error concealment results, the outlier pruning property guarantees the significant quality improvements, both quantitatively and qualitatively. No intermediate user-interaction is required for the pre-segmented media and the presented method follows a bootstrapping approach for an automatic visual loss recovery and the image and video error concealment.

Keywords—Exemplar-based image and video inpainting, outlier pruning, RST-invariant partial patch matching model (RSTI-PPMM), visual error concealment.

I. Introduction

WHILE transmitting images and videos over error prone channels, the data may suffer from losses and errors. Therefore error control is vital for the transmission of images and videos over unreliable (noisy and or lossy) networks and error prone channels, particularly wireless channels. Two possible methods have been proposed in the literature for error control at the receiver end. The first method is based on the automatic retransmission request (ARQ) approach [1], [2], and the other performs by recovering the corrupted information using the correctly received data [3]–[7]. For error recovery using later method two general approaches have been proposed; the error resilient methods (ERM) [3]–[5], and the error concealment methods (ECM) [6], [7]. Among these techniques while the ARQ based methods suffers from the imposed retransmission delays (impractical for many real-time applications), the ERMs add some redundant information to the original data at the transmitter side so as to employ these bits of information for error control/recovery at the receiver end, whenever an error occurs. Since an improved error resiliency necessitates the addition of more extra and redundant information therefore, obviously, ERMs are in contrast with the compression purposes and increase the bandwidth limitations. ECMs however exploit and employ the inherent spatial, spectral, temporal, or hybrid (any combination of these) properties and redundancies of the received data to conceal the error. Hence, in contrast with the ARQs and ERMs, these methods neither add any kind of redundant information nor introduce transmission delays to affect the practicality. Although some times it is achieved at the cost of quality and comparatively higher computational complexity at the receiver end yet these methods can meet the practical (some times even promising) requirements. Furthermore ECMs can also be used together with ERMs and/or ARQs in the situations when either or both of these fail to overcome the errors [8]. Therefore, ECMs have gained an increased research interest in the literature and applications. Here we present an exemplar-based spatial error concealment method working on the principles of the artistic visual media restoration and inpainting. The visual data often possesses a higher level of data redundancy and the available visual media components provide reasonably enough cues about the structural completion of the occluded or the lost regions Therefore, we utilize and exploit these properties to establish a novel exemplar-based error-concealment method. In the scenario of error concealment, the error detection and the media segmentation are among the preliminary and the prerequisite steps. Under the assumptions that the error region is already detected and the media is segmented and labeled into two distinct parts, the source (or the intact) part Ω^c and the target (or the lost) part Ω, we focus our attention to the recovery of the erroneous region(s) only. A lot of research work has already addressed the topics of error detection and media segmentation by using a variety of different algorithms, and discussing the associated algorithmic complexity and/or the performance issues. Therefore these topics are beyond the scope of the presented work.

Media restoration order is evidently crucial to the non-parametric texture synthesis [9] and depends on several different factors. The fundamental factors involved in the texture synthesis include: (a) the spatial and/or spatio-temporal proximities (within a suitable width abutting band around the target region); (b) the number of more available neighbouring pixels; and (c) the local structural details and the texture characteristics, such as the propagating edge features, which directly affect the target region restoration order. As the neighbouring known pixels around the missing region, which is to be recovered and restored, provide the most relevant information about the target region therefore it is quite natural to start filling the target region from the source-target boundary to inward the target region. In this regard the onion-peel method had previously been a favourite choice. Instead of literally

Shiraz Ahmad is with the Department of Electronics and Information Engineering, Harbin Institute of Technology Shenzhen Graduate School, Shenzhen 518055, P. R. China, on leave from Pakistan Atomic Energy Commission (PAEC), Islamabad 44000, Pakistan (phone: 0086-159-1948-1345; fax: 0086-755-2603-3608; e-mail: shiraz_shiraz@yahoo.com).

Zhe-Ming Lu is with the School of Aeronautics and Astronautics, Zhejiang University, Hangzhou 310027, P. R. China (e-mail: zheminglu@zju.edu.cn, zmlu1974@gmail.com).

following an onion-peel method, an isophote driven alternative approach was also proposed in [10]. However, while using the idea of confidence (or belief) term as in [10] here we introduce a new and better RSTI-PPMM for ranking the best matching exemplar. This RSTI-PPMM not only helps in finding the successively improved fill-order priorities but also facilitates the process of a more realistic texture synthesis, for the purpose of error concealment, through an improved partial patch matching model with an inherent outlier pruning characteristic. Furthermore, the specialty of the presented RSTI-PPMM lies in its utility and effectiveness for both the spatial and the spatio-temporal domains, depending upon the usage for static and/or motion imagery. The structural completion order is jointly determined by: (a) the confidence term and the successive belief propagation of the image values, and (b) the evaluation of the rank values for partial patch matching at the specific positions. After finding the fill-order priorities, the final texture synthesis and the error concealment is performed by exemplar-based partial patch replacement mechanism via minimizing the weighted sum of squared differences (SSD) between the target and the source.

II. The Proposed Method

The underlying processes involved in the proposed method include: (a) finding the fill-order priorities for the target region, (b) determination of the confidence values for the target region, (c) rank evaluation by using an exemplar-based RST-invariant partial patch matching model to find the best matching exemplar, and (d) the error concealment and media restoration. The respective descriptions and the underlying details of these processes are presented in the following subsections.

A. Finding the Fill-Order Priorities for the Target Region

Let the image or the visual media $I \in \Re^2$ is represented by the region Φ (defined over domain Ψ), the error region is represented by $\Omega \subset \Phi$, and the unaltered region or the intact media part is represented by $\Omega^c = \Phi \setminus \Omega$ (i.e., $\Omega \cup \Omega^c = \Phi$ and $\Omega \cap \Omega^c = \emptyset$), as shown in Fig. 1. To find the fill-order priorities, for the purpose of error concealment, let us choose a point $\alpha_o \in P_\alpha$ (say the centre of the patch P_α - though other choices are also possible) on the boundary $\partial\Omega$ of Ω, provided that $\partial\Omega \notin \Omega$. The point $\alpha_o \in P_\alpha$ is chosen such that a part of the patch P_α belongs to the region Ω whereas the rest belongs to the region Ω^c, enclosed in an abutting band B.

The width of the band B is chosen as an appropriate multiple of the size of the patch P_α. It is also straightforward to consider that the values beyond the region B are not very useful because the local structural details seldom extend over the large regions or the entire visual domain. Furthermore, the patch can also be chosen in any suitable shape (such as square, circle, or diamond) and a reasonable size. As a matter of choice, choosing a patch in a square shape is more straightforward and easier to handle. Therefore, for the sake of simplicity we also use a square patch with a 9×9 pixel size.

In order to achieve a good compatibility advantage during the error concealment process, we prioritize the selection of the starting point α_o such that: (a) most of the neighbors of the point α_o in the patch P_α are known, and (b) there are some local structural details, such as an edge or gradient, within the patch P_α. After finding a suitable starting point, the successive fill-order or restoration priorities are computed by suing the following relation.

$$\mathbb{P}(\alpha_o) = \mathbb{C}(\alpha_o) rank(\alpha_o) \tag{1}$$

where $\mathbb{C}(\alpha_o)$ is the confidence term or the belief value, same as used in [10], and $rank(\alpha_o) \in [0, 1]$ gives the compatibility of the patch P_α (around α_o) with the patch P_β.

B. Determination of the Confidence Values for the Target Region

Since the known pixel values refer to the source region and the corrupted or missing pixel values correspond to the target region(s), therefore, the natural way of belief upon the values of these two regions is to consider and assign the highest confidence to the available source region whilst the lowest confidence for the target corrupted or missing region. Hence, in the beginning, the belief values are initialized and assigned based on this notion, as given by using the relation:

$$\mathbb{C}(\alpha_o) = \begin{cases} 0 & \forall \alpha_o \in \Omega \\ 1 & otherwise \end{cases} \tag{2}$$

Since the belief value serve as a critical measure of the amount of reliable information surrounding a pixel therefore already known neighboring pixels play the direct role in early determination, computation, and initialization of the belief values. Following the similar approach, the successive belief values are jointly determined by using the already determined confidence values, and so on, until assigning a confidence value to the whole media. In general, the overall and successively determined confidence or belief in the value of any potential pixel can be calculated by using the confidence information of its neighboring pixels. Mathematically, the confidence value at an intermediate stage can be calculated by using the following relation.

$$\mathbb{C}(\alpha_o) = \frac{\sum_{\alpha_i \in P_\alpha^{\Omega^c}} \mathbb{C}(\alpha_i)}{|P_\alpha|} \tag{3}$$

where $\alpha_o \in P_\alpha$ is the point under consideration, $\alpha_i \in P_\alpha^{\Omega^c}$ represent the available or known neighboring pixels of α_o in the patch P_α, $|P_\alpha|$ represents the size of the patch, and $\mathbb{C}(\alpha_o)$ gives the confidence at point α_o over the patch P_α.

It is to be noted that the target region points adjoining the boundary $\partial\Omega$ have more known and available neighbors, therefore they assume higher belief values. Similarly the points for which the confidence values have already been determined in the earlier steps have direct affect and contribution to the determination of the successive belief values. In this way the points around the outer rim of the region Ω gain the higher belief values than the more inner parts. Subsequently, the successive belief values are computed and updated in the same fashion, as in [10].

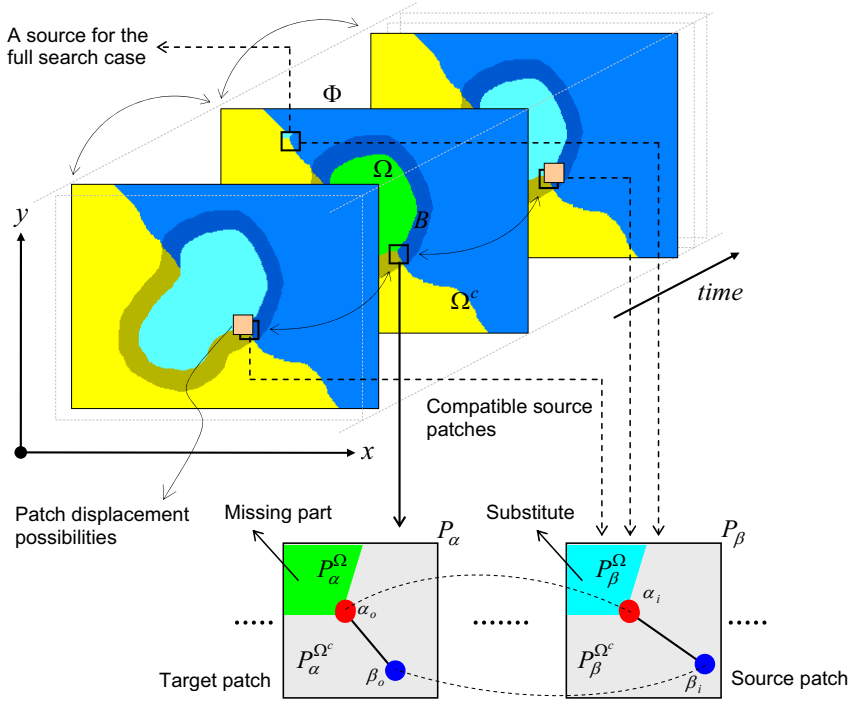

Fig. 1: The patch compatibility illustration in the spatial and the spatio-temporal domains

C. Rank Evaluation by using an Exemplar-based RST-Invariant Partial Patch Matching Model (RSTI-PPMM)

We employ an RSTI-PPMM to compute the patch rank in the spatial or spatio-temporal domain by using an arbitrary pair of known feature points, as depicted in Fig. 1. Let us choose a patch P_α, around the high priority starting point (which assumes an initial higher confidence value), such that the chosen patch partially belongs to both of the target Ω and the source region Ω^c. We compute the rank or compatibility of a patch in terms of the availability of a good exemplar-based partial match for it from within the source. For this purpose we perform a partial patch matching of the patch P_α with the patches from within the source such that the available pixels of the patch P_α contribute to this matching. For a more closer matching a higher rank value is achieved and during error concealment the media restoration process is prioritized accordingly, based on the higher rank values. Because of different kinds of potential scaling, rotation, or other orientation possibilities several measure are needed to be considered and involved so as to have an improved matching model. Therefore, we take the potential factors into account by presenting a rotation, scale, and translation-invariant partial patch matching model which is capable not only to perform the partial patch matching but can also handle the outliers or the missing feature points during the course of patch matching and the corresponding rank evaluation.

Let for a pair of analogous vertices (α_o, α_i) and (β_o, β_i), the patches P_α and P_β are related by Q and W, where $Q(\angle, D)$ contains the angle and the length of the vector linking the two components from distinct features, and $W(rS, rO)$ contains the relative scale and orientation between two component features. The patch rank is computed by checking the compatibility of the patch P_α with the patch P_β in terms of the scale, orientation, and the vector angle and the length. The details about the computation of the corresponding intermediate ranks based on these measures are presented as below.

The measure of the rank for the relative scales of the corresponding pair of features in the two patches P_α and P_β is given by:

$$\triangle S^{o,i} = 1 - \frac{|rS(\beta_o, \beta_i) - rS(\alpha_o, \alpha_i)|}{rS(\alpha_o, \alpha_i) + rS(\beta_o, \beta_i)} \tag{4}$$

where $rS(\circ, \bullet)$ represents the relative scale connecting the vertices $\circ$ and $\bullet$.

Let for the sake of simplicity we use the notation as,

$$X(a_k, b_l) = X_{a_k, b_l} \tag{5}$$

then (4) can be re-written in the simplified form as:

$$\triangle S^{o,i} = 1 - \frac{|rS_{\beta_o,\beta_i} - rS_{\alpha_o,\alpha_i}|}{rS_{\alpha_o,\alpha_i} + rS_{\beta_o,\beta_i}} \tag{6}$$

Similarly, the measure of the rank for the relative orientation within the pair of features is given by:

$$\triangle O^{o,i} = 1 - \frac{\hat{O}|rO_{\beta_o,\beta_i} - rO_{\alpha_o,\alpha_i}|}{180} \tag{7}$$

where $\hat{O}(x)$ is used as the normalization function, to take into account the fact that the orientations are measured in a closed circle, as given by:

$$\hat{O}(x) = \begin{cases} 360 - x, & if \quad x > 180 \\ x, & otherwise \end{cases} \tag{8}$$

It is to be noted that apart from the rotation that each feature pair suffers from one patch to the other, the angle of vectors connecting the features in the corresponding patches is expected to be preserved. Therefore to find the best estimate for the angle in the corresponding patches we compute the two differences and take the minimum between these differences, as given by:

$$\triangle\angle^{o,i} = 1 - \frac{MIN|\hat{O}(d\angle_{\alpha}^{o,i}), \hat{O}(d\angle_{\beta}^{o,i})|}{180} \tag{9}$$

where $\hat{O}$ is the same normalization function, as given above, to keep the measurements within the closed circle, and the two differences $d\angle_{\alpha}^{o,i}$ and $d\angle_{\beta}^{o,i}$ are given by:

$$d\angle_{\alpha}^{o,i} = |\angle_{\alpha_i,\beta_i} - (rO_{\alpha_o,\alpha_i} + \angle_{\alpha_o,\beta_o})| \tag{10}$$

$$d\angle_{\beta}^{o,i} = |\angle_{\alpha_i,\beta_i} - (rO_{\beta_o,\beta_i} + \angle_{\alpha_o,\beta_o})| \tag{11}$$

Similarly, the measure of the rank for the relative estimate of the lengths of vectors is given by:

$$\triangle D^{o,i} = 1 - \frac{MIN(dD_{\alpha}^{o,i}, dD_{\beta}^{o,i})}{q^{o,i}} \tag{12}$$

here the terms appearing in (12) are given by:

$$dD_{\alpha}^{o,i} = |D_{\alpha_i,\beta_i} - (rS_{\alpha_o,\alpha_i} \times D_{\alpha_o,\beta_o})| \tag{13}$$

$$dD_{\beta}^{o,i} = |D_{\alpha_i,\beta_i} - (rS_{\beta_o,\beta_i} \times D_{\alpha_o,\beta_o})| \tag{14}$$

$$q^{o,i} = \begin{cases} D_{\alpha_i,\beta_i} + (rS_{\alpha_o,\alpha_i} \times D_{\alpha_o,\beta_o}), & if \quad dD_{\alpha}^{o,i} < dD_{\beta}^{o,i} \\ D_{\alpha_i,\beta_i} + (rS_{\beta_o,\beta_i} \times D_{\alpha_o,\beta_o}), & otherwise \end{cases} \tag{15}$$

Similar to the angle comparison and apart from the change in the scale from one patch to the other, the lengths of vectors connecting the two features in the corresponding patches should be preserved.

In order to compute a more unified compatibility measure and to find an overall patch rank value there are two possible approaches of combining all these intermediate rank values ($\triangle S^{o,i}$, $\triangle O^{o,i}$, $\triangle\angle^{o,i}$ and $\triangle D^{o,i}$) together into a single quantity, as described and presented below. One approach is to combine them all additively through averaging, as given by (16), whereas the other way is to combine them multiplicatively, as given by (17). However, both approaches have their own pros and cons offering different levels of compromise. For example, if the final rank value is computed multiplicatively then the presence of a single null value can make the whole estimate zero. An alternative and a more conservative approach is via averaging. However, the risks involved in this approach are that some of the completely out of place features will be included too. In this way computation of the overall rank value will be directly affected, leading to a significant accuracy compromise.

In order to achieve an improved accuracy and to make the model as precise as possible we exclude the affect of the missing feature points by performing the outlier pruning. The outliers are interpreted as the missing feature points (such as noises) and we deal with them through the introduction of a wild-card feature, represented by the symbol "$*$". During the outlier pruning, we simply discard the feature pairings (marked with $*$'s) for which the computations can not be performed based on the real image evidence. Therefore, when performing computations the outliers or the missing feature points marked with $*$'s are not taken into account. In this way, the overall rank values by using either the additive or the multiplicative case can respectively be given as follows.

$$rank(\alpha_o) = \sum_{\forall\alpha,\beta\in 1,\ldots,N} \frac{\triangle S^{o,i} + \triangle O^{o,i} + \triangle\angle^{o,i} + \triangle D^{o,i}}{2 \times N \times (N-1)} \tag{16}$$

$$rank(\alpha_o) = [\prod_{\alpha=1}^{N-1} \prod_{\beta=\alpha+1}^{N} \triangle S^{o,i} \triangle O^{o,i} \triangle\angle^{o,i} \triangle D^{o,i}]^{\frac{1}{\lambda}} \tag{17}$$

here α_o, α_1, β_o, $\beta_i \neq *$, N is the number of analyzed patches, and the term λ in the exponent is the normalization term involving only the available feature pairings.

The typical intermediate rank values fall within the open interval $(0, 1)$, i.e., for all of the intermediate rank values we have $\triangle S^{o,i}$, $\triangle O^{o,i}$, $\triangle\angle^{o,i}$, $\triangle D^{o,i} \in (0, 1)$. Furthermore, it is important to notice that for a better overall patch compatibility all of the intermediate ranks should assume higher values. However, as the number of analyzed patches in (17) increase, the final rank value tends to decrease exponentially towards zero. This is due to the reason that typically the intermediate rank values fall within the open interval $(0, 1)$. This problem of fast rank decay can be handled by using the normalization wrapper λ. This normalization term in the exponent involves only the total number of available feature pairings for which the computation can be performed on the real image evidence. We simply discard the feature pairings which have at least one wild card, since the computations can not be performed for these pairs. Thus the normalization term λ is computed as the difference of the total number of possible feature pairings and the total number of pairings involving outliers, i.e.,

$$\lambda = a - b \tag{18}$$

where we have,

$$a = total\,\#.\,of\,possible\,pairings = \frac{N(N-1)}{2} \tag{19}$$

and

$$\begin{aligned} b &= total\,\#.\,of\,pairings\,with\,*'s \\ &= \frac{nW(\alpha,\beta)[2N - nW(\alpha,\beta) - 1]}{2} \end{aligned} \tag{20}$$

Mathematically this term can now be re-written as:

$$\lambda = \frac{N(N-1)}{2} - \frac{nW(\alpha,\beta)[2N - nW(\alpha,\beta) - 1]}{2} \tag{21}$$

where N is the number of the scene images analyzed and the function $nW(\alpha, \beta)$ recognizes the total number of $*$'s found

in either α or β, as given by:

$$nW(\alpha,\beta) = \sum_{i=1}^{N} voidW(\alpha_i,\beta_i) \tag{22}$$

with

$$voidW(\alpha_i,\beta_i) = \begin{cases} 1 & if\ any\ of\ \alpha\ or\ \beta\ is\ missing \\ 0 & otherwise \end{cases} \tag{23}$$

Since the affect of $*$'s can be avoided through outlier pruning therefore, as a matter of choice, we choose to use the multiplicative approach as given by (17).

D. Error Concealment and Media Restoration

After computing the fill order priorities, error concealment is started from the highest priority regions. In [9] and [10] authors performed the direct sampling of the source region and minimized the sum of squared difference (SSD) between the target and the source pixel intensity values. However, the neighborhood of Ω can also contain noise or missing feature points. Therefore, using all of the neighbours irrespective of whether they may contain noise or not, is not be a good choice and can yield undesired results. In order to avoid this situation we define a new weighted-SSD (WSSD) which not only takes into account the scattered outliers but can also handle the partial neighbours. While taking into account the partial neighbours and considering the scattered outliers, the WSSD for the two correspondingly available vertices $\hat{\alpha}_o$ and $\hat{\alpha}_i$, respectively belonging to two different compatible patches, is computed as follows.

$$d(P_\alpha^{\Omega^c}, P_\beta^{\Omega^c}) = \frac{\sum_{\hat{\alpha}_o \in P_\alpha, \hat{\alpha}_i \in P_\beta} \mathbb{C}(\hat{\alpha}_o)\mathbb{C}(\hat{\alpha}_i)[\mathbb{I}(\hat{\alpha}_o) - \mathbb{I}(\hat{\alpha}_i)]^2}{[\sum_{\hat{\alpha}_o \in P_\alpha, \hat{\alpha}_i \in P_\beta} \mathbb{C}(\hat{\alpha}_o)\mathbb{C}(\hat{\alpha}_i)]^2} \tag{24}$$

For faster computations and plausible texture synthesis, we utilize the previously determined high rank patches. Finally we find the suitable substitute P_β^Ω for P_α^Ω through minimizing the WSSD, by using the relationship:

$$P_\alpha^\Omega = \arg\min\ d(P_\alpha^{\Omega^c}, P_\beta^{\Omega^c}) \tag{25}$$

III. Results and Discussion

Under prior media segmentation assumption, our method follows a bootstrapping approach for automatic concealment of the visual errors by following an exemplar-based inpainting approach. The effectiveness of the proposed method has been tested for one image (Fruits) and the two videos [11]. The video-1 named "A new horizon" is sampled at the rate of 10 frames-per-second (fps), whereas the video-2 named "The great web of water" is sampled at the rate of 5 fps, by using a non-optimized implementation. In order to check the success of the proposed method, here the attention has been paid only to the error concealment part and the computational complexity and/or the performance related issues are not considered. The pre-segmented media and the error concealment results (for the fruits image, the frame 23 of the video-1, and the frame 164 of the video-2) are shown in Fig. 2, and presented in Table I.

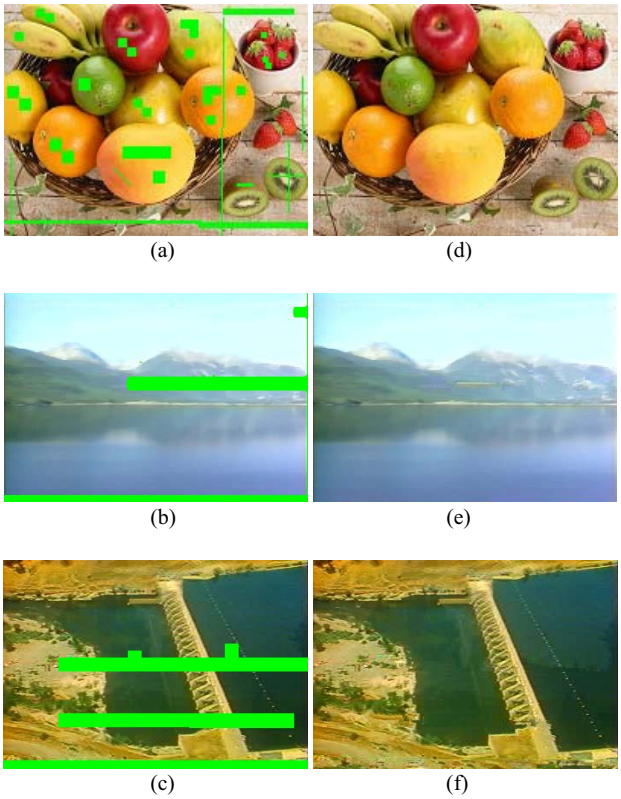

Fig. 2: Experimental results; (a)-(c) present the segmentation results of the corrupted media, and (d)-(f) present the recovered media after visual error concealment via exemplar-based inpainting.

TABLE I
PSNR Improvement in the Image and Video Error Concealment

Description of the media		The size of error in the image or video frame measured in		PSNR gain/ improvement
Type	Size (in pixels)	in # of pixels	percentage	(in db)
Fruits image	200 × 150	2,220	7.400 %	18.028
Video – 1 (@5 fps)	352 × 240	6,594	7.805 %	11.990
Video – 2 (@10 fps)	352 × 240	12,985	15.370 %	13.829

From Fig. 2 it can clearly be seen that the visual error concealment results are not only perceptually plausible but the values for the peak signal-to-noise ratios (PSNRs) are also significantly improved, as presented in Table I.

A comparison of our scheme with the classical inpainting technique of Criminisi, Perez, and Toyama is also presented in Table II. The given results also show that our proposed method achieves a significant PSNR improvement resulting in a better

TABLE II
COMPARISON BETWEEN THE ERROR CONCEALMENT RESULTS USING THE PROPOSED METHOD AND THE CLASSICAL EXEMPLAR-BASED INPAINTING METHOD OF CRIMINISI, PEREZ, AND TOYAMA [10]

Description of the media	PSNR gain/improvement (in db)	
	Proposed method	Method of Criminisi, Perez and Toyama
Fruits image	18.028	12.281
Video – 1	11.990	7.627
Video – 2	13.829	9.608

gain in comparison to their method.

It is also to be noted that the computational complexity can effectively be reduced and a good quality-performance balance can be achieved by: (a) a suitable selection of the patch size, depending upon the media at hand and varying from situation to situation; (b) limiting the number of compatibility measures in (16) or (17); and (c) the proper outlier pruning.

IV. CONCLUSION

This paper presents a novel and effective visual error concealment method, for the images and video, utilizing the principle of exemplar-based inpainting. For an error detected and pre-segmented media no intermediate user-interaction is required and the method follows a bootstrapping approach for the automatic concealment of the visual error. The presented RST-invariant partial patch matching model (with an inherent outlier pruning characteristic) ensures finding the robust exemplars for synthesis of the target missing regions. Furthermore, the computational burden can also effectively be reduced with an intelligent control and reduction of the search space. Consequently, a more realistic, perceptually plausible, and greatly improved (both quantitatively and qualitatively) error concealment is achieved. In addition to this, and beside error concealment, our method can also be used and realized for several other purposes and applications such as: disocclusion, visible watermark removal, object removal, image and video crack removal, visual scene editing, special effect creation, compression, etc.

ACKNOWLEDGMENT

This work is supported by "The Fifty (50) Excellent Talent Support Scheme" of the Higher Education Commission (HEC), Pakistan; Pakistan Atomic Energy Commission (PAEC), Pakistan; and the "New Century Excellent Talents in the Universities of China" under the grant number NCET-04-0329. Special thanks are due to Mr. Bin Cao for the generous help and support in the LaTeX typesetting.

REFERENCES

[1] S. Lin, D. J. Costello, and M. J. Miller, "Automatic repeat request error control schemes," *IEEE Communication Magazine*, vol. 22, no. 12, pp. 5-17, 1984.

[2] B. Girod and N. Farber, "Feedback-based error control for mobile video transmission," *Proc. IEEE*, vol. 87, no. 10, pp. 1707-1717, 1999.

[3] J. Hagenauer and T. Stockhammer, "Channel coding and transmission aspects for wireless multimedia," *Proc. IEEE*, vol. 87, no. 10, pp. 1764-1777, 1999.

[4] S. B. Wicker, *Error control systems for digital communication and storage*, Upper Saddle River, NJ: Prentice-Hall, 1995, ch. 15.

[5] V. K. Goyal, "Multiple description coding: compression meets the network," *IEEE Signal Processing Magazine*, vol. 18, no. 5, pp.74-93, Sept. 2001.

[6] B.W. Wah, X. Su, and D. Lin, "A survey of error-concealment schemes for real-time audio and video transmission over the internet," *in Proc. IEEE Int. Symp. Microelectronic Systems Education*, Taipei, Taiwan, 2000, pp. 17-24.

[7] P. Cuenca, L. Orozco-Barbosa, A. Garrido, F. Quiles, and T. Olivares, "A survey of error concealment schemes for MPEG-2 video communications over ATM Network," *in Proc. IEEE Canadian Conf. Electrical and Computer Engineering*, St John's, NF, Canada, 1997, vol. 1, pp. 118-121.

[8] M. Bystrom, V. Parthasarathy, and J. W. Modestino, "Hybrid error concealment schemes for broadcast video transmission over ATM networks," *IEEE Trans. Circuits, Syst. and Video Tech.*, vol. 9, no. 6, pp. 868-881, Sept. 1999.

[9] A. A. Efros and T. K. Leung, "Texture synthesis by non-parametric sampling," *in Proc. 7th Int. Conf. Computer Vision*, Kerkyra, Corfu, Greece, 1999, pp. 1033-1038.

[10] A. Criminisi, P. Perez, and K. Toyama, "Region filling and object removal by exemplar-based inpainting," *IEEE Trans. Image Processing*, vol. 13, no. 9, pp. 1200-1212, Sept. 2004.

[11] OV: The open video project - a shared digital video collection. Available: http://www.open-video.org